CrossMark

Measurement of cortical thickness asymmetry in carotid occlusive disease

Iris Asllani[a,*], Pamelia Slattery[a], Alexander Fafard[a], Marykay Pavol[b], Ronald M Lazar[b], Randolph S Marshall[b]

[a]Rochester Institute of Technology, New York, USA
[b]Columbia University Medical Center, USA

ABSTRACT

Despite being considered an important anatomical parameter directly related to neuronal density, cortical thickness is not routinely assessed in studies of the human brain *in vivo*. This paucity has been largely due to the size and convoluted shape of the human cortex, which has made it difficult to develop automated algorithms that can measure cortical thickness efficiently and reliably. Since the development of such an algorithm by Fischl and Dale in 2000, the number of studies investigating the relationship between cortical thickness and other physiological parameters in the brain has been on the rise. There have been no studies however that have validated cortical asymmetry against known vascular anatomy. To this aim, using high-resolution MRI, we measured cortical thickness and volume in the primary motor (M1) and primary visual (V1) cortex in patients with unilateral, high-grade carotid occlusive disease (n = 29, age = 74 ± 10 years). These regions were selected based on the hypothesis that there will be thinning of the cortical thickness of M1 in the territory supplied by the occluded carotid artery, whereas V1 will show no asymmetry since its blood supply is provided by unaffected posterior arteries. To test for an effect of handedness, cortical thickness and volume were also measured in healthy volunteers (n = 8, age = 37 ± 13 years). In patients, we found thinner cortex in M1 on the occluded side (mean = 2.07 ± 0.19 mm *vs* 2.15 ± 0.20 mm, p = 0.0008) but no hemispheric difference in V1 (1.80 ± 0.17 mm in occluded *vs* 1.78 ± 0.16 mm in unoccluded, p = 0.31). Although the mean cortical volume of M1 in the occluded hemisphere was also lower, the difference did not reach statistical significance (p = 0.09). Similarly, in healthy controls, the results showed no hemispheric asymmetry in either cortical thickness or volume in either region (p > 0.1). To test for an orientation bias in the method, the analysis was repeated with images flipped from neurological to radiological orientation. While the algorithm did not yield identical results for the two orientations, the effect did not alter the findings of the study. These results provide a method for within-subject validation of a pathophysiological effect of carotid occlusive disease on the human cortex and warrant further investigation for underlying mechanisms.

1. Introduction

Imaging studies have consistently shown that normal aging and disease are associated with structural changes in the cerebral cortex. These changes are commonly assessed as changes in volume rather than in cortical thickness despite indications that cortical thinning might represent a more specific marker of post-injury or degenerative processes (Fotiadis et al., 2016; Geisseler et al., 2016; Hwang et al., 2016).

Cortical thickness is typically defined as the average distance between the white matter surface and the pial surface, which can be computed locally, over a region of interest (ROI), or globally, over a hemisphere and the entire brain (Fischl and Dale, 2000). Historically, *in vivo* measurement of cortical thickness of functional regions in the brain has been difficult because of the complexities of the shape and size of the human cortex. Until relatively recently, the most viable option was manual delineation of the cortical regions, a method both time-consuming and unreliable for cross-study comparisons (Desikan et al., 2006).

In 2000, Fischl and Dale developed Freesurfer, an automated surface-based method (Fischl and Dale, 2000) for measuring cortical thickness that has since been validated against histological analysis (Rosas et al., 2002) as well as manual measurements (Kuperberg et al., 2003; Salat et al., 2004). In addition, the method has been shown to produce reliable test-retest estimates across scanner types and field strengths (Han et al., 2006; Reuter et al., 2012). In tandem with the validation studies, an increasing number of studies have used the cortical thickness measurement as a correlate of physiological changes in the brain in normal aging and disease (Han et al., 2006; Kuperberg et al., 2003; Sailer et al., 2003; Rosas et al., 2003).

Nonetheless, the method is relatively new, and further independent studies are needed to test its reliability and clinical usefulness. In

* Corresponding author.
E-mail address: icabme@rit.edu (I. Asllani).

particular, although cortical thinning has been reported in several recent studies with focal pathology (Cheng et al., 2015; Duering et al., 2015), there have been no controlled studies for cerebrovascular diseases that take advantage of known vascular anatomy.

In this study, we used high-resolution anatomical MRI images to test for hemispheric asymmetry in cortical thickness in asymptomatic patients with unilateral carotid occlusive disease. This condition provides a robust model for testing regional cortical thinning in the vascular territory directly affected by the occlusion. We tested the hypothesis that there would be thinning of the primary motor cortex (M1) on the side of the occluded artery, but no hemispheric asymmetry in cortical thickness of V1, since the visual cortex receives its blood supply from the unoccluded posterior cerebral arteries. Such a finding would validate cortical thickness measurements as a biomarker for regional or focal vascular disease, providing support for future studies of vascular pathophysiology and its functional correlates.

2. Methods

2.1. Study participants

2.1.1. Patients

Twenty-nine patients, age 50–93, 19 male, 26 right-handed, with unilateral 80–100% ICA occlusion but no stroke were enrolled in the study. Out of the 29 patients, 16 (55%) had their occlusion on the left side. Inclusion criteria were: ≥80% carotid stenosis or complete occlusion by carotid Doppler, MRA, or CTA, with <40% stenosis in the contralateral ICA. Other inclusion criteria were: asymptomatic status or TIA-only referable to the ICA stenosis, fluent in English, and able to give informed consent. Exclusion criteria included prior clinical stroke, diagnosis of dementia, history of moderate-severe head trauma, current substance abuse, major psychiatric disease, NYHA Stage 3/4 congestive heart disease, or contraindication to MRI.

2.1.2. Healthy controls

As an additional control for hemispheric asymmetry in the selected ROIs, we analyzed images acquired on eight right-handed healthy volunteers, age 21–56, 4 male, enrolled for a different study conducted by one of the authors (IA) at the Leiden University Medical Center.

All participants signed the consent form approved by the respective institutions' ethics review board.

2.2. Image acquisition and processing

Imaging was performed on 3T Philips Achieva scanners in the medical centers of Columbia University (patients) and Leiden University (healthy controls). A high-resolution 3D T1-weighted (MPRAGE) image was acquired on each participant with the following parameters: TE = 3 ms, TR = 6.7 ms, in plane resolution 0.9×0.9 mm^2, slice thickness = 0.9 mm, 120 slices. An in-house SPM12 (Wellcome Trust Centre for Neuroimaging, London, UK) based script was used to flip the orientation of the images such that they were available in both neurological and radiological orientations. This was done to test for any orientation bias in Freesurfer's performance of cortical thickness estimation.

Volumetric tissue segmentation and inference of cortical structure were obtained from each patient's MPRAGE (neurological and radiological orientation, independently) using the Freesurfer software (Fischl and Dale, 2000).

Briefly, the Freesurfer approach involved: (1) removal of non-tissue voxels using a hybridized watershed/surface deformation algorithm (Ségonne et al., 2004), (2) computation of forward and inverse transforms into Talairach space, (3) volumetric segmentation of subcortical white matter and deep gray matter structures (Fischl et al., 2002; Fischl et al., 2004), (4) intensity normalization (Sled et al., 1998), (5) tessellation of the boundary between gray and white matter, (6) automated topology correction (Fischl et al., 2001; Ségonne et al., 2007),

and (7) surface deformation, which is conducted along intensity gradients such that transitional borders are positioned along the greatest shift in signal intensity aligned with the border to the next tissue class (Dale et al., 1999; Dale and Sereno, 1993; Fischl and Dale, 2000).

Following the registration to a spherical brain atlas utilizing cortical folding patterns of subjects to match cortical geometry across subjects (Fischl et al., 1999), the cerebral cortex was parcellated into different regions based on the structure of the gyri and sulci (Desikan et al., 2006; Fischl et al., 2004). With both the inner and outer cortical surfaces identified and isolated, the cortical thickness of a subject was calculated as the Euclidean distance between the two surfaces (Fischl and Dale, 2000).

The cortical thickness maps are created through the use of spatial intensity gradients across tissue classes and are therefore largely invariant to absolute signal intensity.

Based on the parcellation results, regions of interest were selected for the cortical thickness map of the primary motor cortex (M1) and primary visual cortex (V1). Data from these ROIs were used to compute cortical thickness and volume, which were subsequently used in the analysis described below.

2.3. Data analyses

The cortical thickness (CT) coefficient of asymmetry between hemispheres was defined as

$$C_a = \frac{(CT_{unoccl} - CT_{occl})}{(CT_{unoccl} + CT_{occl})} \cdot 100 \tag{1}$$

where CT_{unoccl} and CT_{occl} denote cortical thickness in the unoccluded and occluded hemispheres, respectively. The coefficient of asymmetry (Eq. (1)) looks at the difference between hemispheres normalized to the sum so that it is not dependent on the mean values of each hemisphere. C_a can take positive values (meaning the cortical thickness of occluded hemisphere is lower), zero (meaning no hemispheric difference) or negative (meaning the cortical thickness is higher in the occluded hemisphere.)

A paired t-test (Bonferroni corrected for multiple comparisons, n = 2, with two tailed $\alpha = \alpha_{uncorr}/2 = 0.025$) was run for cortical thickness and volumetric data in M1 and V1 from each group, independently. The corrected p-values are reported as p_{corr}. The analysis was run twice, once each for neurological and radiological orientations.

3. Results

There was considerable variation in size and shape of both the primary motor (M1) and primary visual (V1) cortex within the same hemisphere across participants as well as between hemispheres on the same participant. Qualitatively, this variation is reflected in Fig. 1, which shows 3D surface rendering of M1 (Fig. 1A) and V1 (Fig. 1B) from six randomly selected patients.

The average cortical thickness of M1 in the hemisphere on the side of the occluded carotid was significantly lower than in the unoccluded hemisphere: 2.07 ± 0.19 mm vs 2.15 ± 0.20 mm ($t_{28} = 3.9$, $p_{corr} = 0.0008$.) Although on average the volume of M1 was also lower in the occluded hemisphere (3399 ± 791 mm^3) compared to the unoccluded (3496 ± 825 mm^3), the effect did not reach statistical significance ($p_{corr} = 0.4$).

In V1 there was no statistical difference in either cortical thickness (1.80 ± 0.17 mm in occluded vs 1.78 ± 0.16 mm in unoccluded, $t_{28} = -1.05$, $p_{corr} = 0.4$) or volume (3410 ± 747 mm^3 vs 3503 ± 698 mm^3, $t_{28} = -0.6$, $p_{corr} = 0.6$).

To give a sense of the hemispheric differences at the individual patient level, the distribution of the coefficient of asymmetry, C_a, across all patients is shown in Fig. 2 for both ROIs. Of the 23 patients with a >1% asymmetry in M1, 19 had lower cortical thickness values on the occluded side.
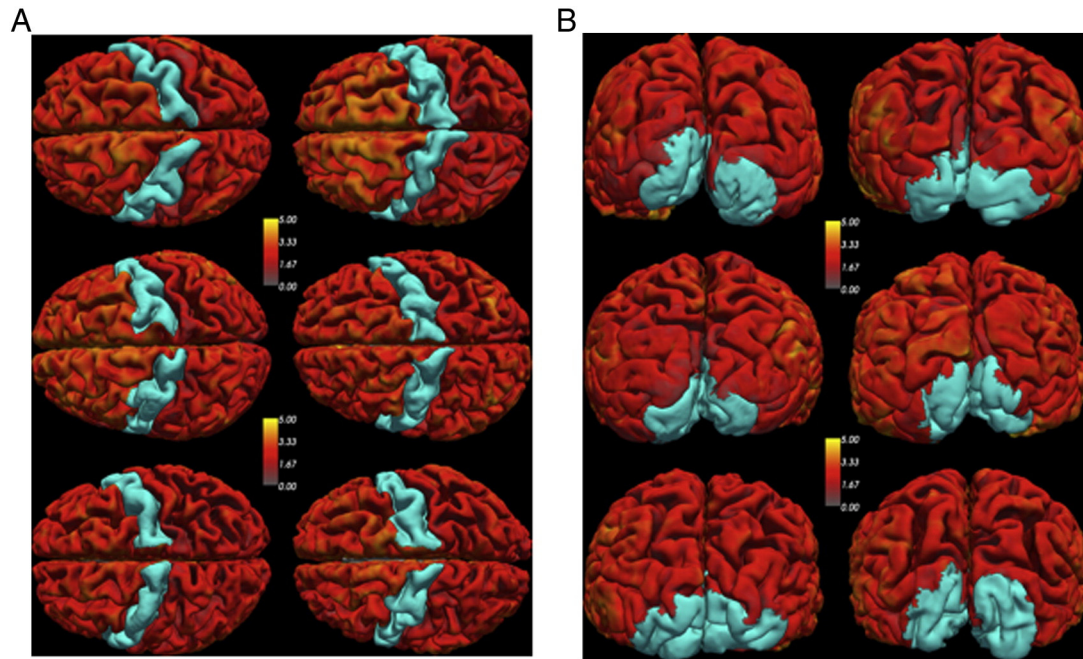
Fig. 1. 3D surface rendering of the primary cortex, M1, (A) and the visual cortex, V1, (B) from 6 randomly selected patients. These regions of interest were extracted from patient's MPRAGE image. Note the variability in size and shape across hemispheres as well as across patients. Cortical thickness asymmetry was measured in M1 (supplied by the carotids), and V1 (not supplied by the carotids).

Among controls, we found no hemispheric asymmetry in either cortical thickness or volume in either ROI. The average cortical thickness of M1 was 2.48 ± 0.17 mm and 2.43 ± 0.12 mm for the left and right hemispheres, respectively, ($p = 0.28$). The corresponding values for the M1 volume were: left hemisphere = 5551 ± 925 mm^3, right hemisphere = 5469 ± 1300 mm^3, ($p = 0.13$).

To test for an orientation bias in the results, the images were flipped from neurological to radiological orientation and the analysis was run anew. While there was clearly an asymmetry by image template orientation (Fig. 3), the cortical thickness of M1 in the occluded hemisphere remained significantly lower than in the unoccluded side ($t_{28} = 3.6$, $p_{corr} = 0.0011$). Similarly, although the distribution of cortical thickness for V1 was not identical between the two image orientations, at the group level, there was no significant difference in cortical thickness estimates across hemispheres.

4. Discussion

Using a unilateral carotid occlusion model, we demonstrated hemispheric asymmetry in cortical thickness of the primary motor cortex, an area of the brain that receives its blood flow directly from the carotid arteries. We further demonstrated the regional specificity of this finding by showing that in the same patients there was no asymmetry in the primary visual cortex, a region that receives its blood supply from the unoccluded posterior circulation and therefore is expected to remain unaffected by the carotid occlusion.

Our finding of a 3.7% decrease in cortical thickness of M1 in unilateral carotid artery disease occurred in the absence of frank stroke, presumably arising from a reduction in blood flow on the occluded side. Prior studies have shown cortical thinning related to subcortical stroke (Cheng et al., 2015; Duering et al., 2015), and in remote white matter lesions in multiple sclerosis (Jehna et al., 2015) but ours is the first to demonstrate this finding from vascular stenosis alone. Although the findings are consistent with the assumption of low blood flow in this carotid occlusion model, this hypothesis remains to be tested.

Although the absolute values of the hemispheral difference seem small, the 3.7% mean difference is not only highly statistically significant, but quite robust when considering the average yearly cortical thinning by age, which is reported to be approximately 0.2% in midlife in normal controls (Shaw et al., 2016) 1.2–1.5% in the hippocampal cortex of older subjects with mild cognitive impairment (Das et al., 2012), and 4.7% in the hippocampal cortex in relatives of Alzheimer's patients
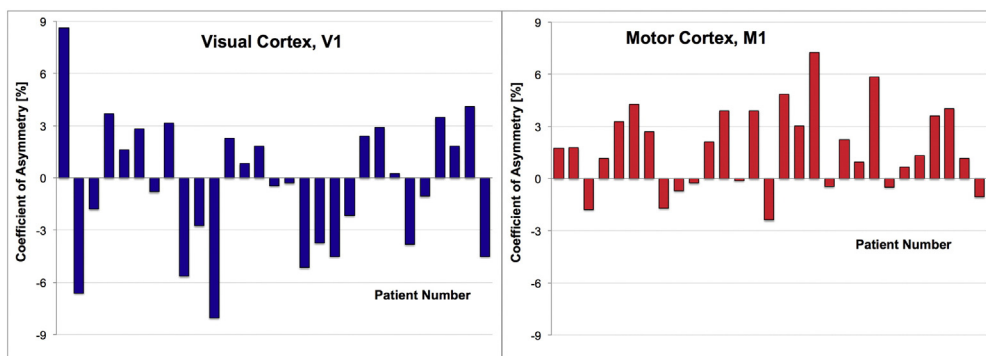
Fig. 2. Distribution of the coefficient of asymmetry (computed as per Eq. (1)) across all patients for the primary motor cortex (right, red) and the primary visual cortex (left, blue). (For interpretation of the references to color in this figure legend, the reader is referred to the web version of this article.)
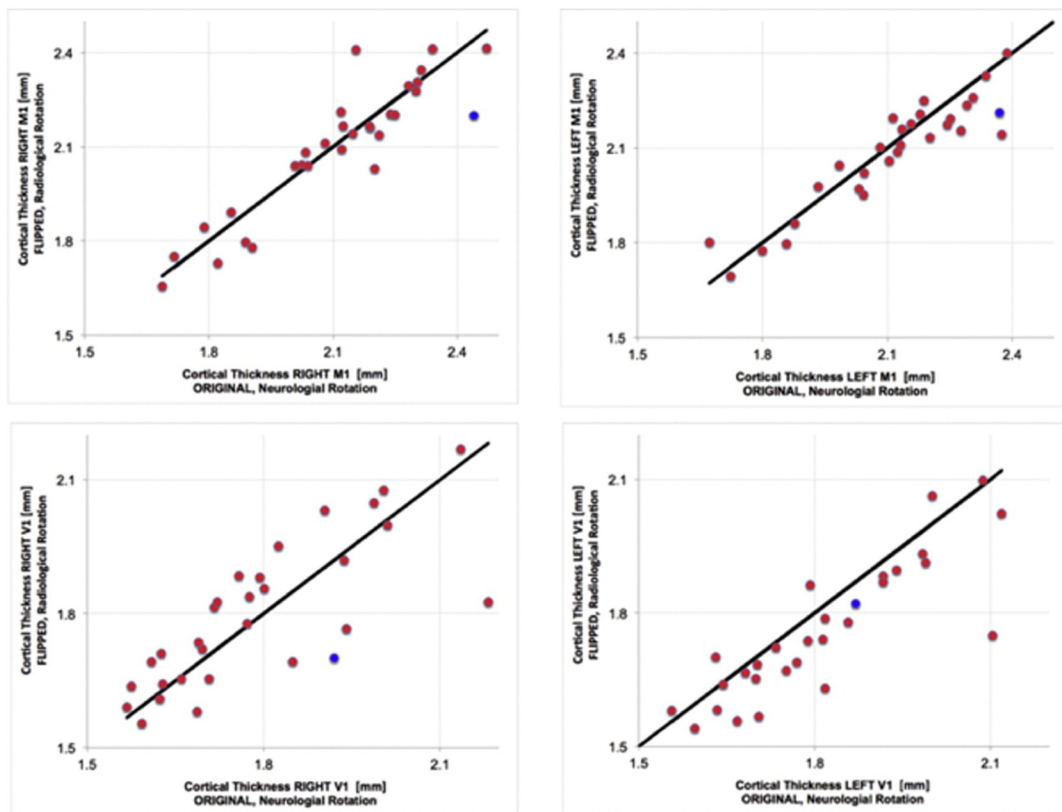
Fig. 3. Effect of image orientation on cortical thickness estimation of M1 (upper) and V1 (lower) for both right and left hemispheres. The solid line represents the identity line. The red dots denote patient data whereas the blue dot was obtained from using the Freesurfer template image. (For interpretation of the references to color in this figure legend, the reader is referred to the web version of this article.)

carrying the APOEε4 allele (Harrison et al., 2016). Thus the absolute differences we are seeing related to carotid occlusion are as much or more than those seen in other pathological subpopulations.

While the findings with cortical thickness were statistically robust, we found no significant difference for cortical volume by hemisphere. We believe this is due the lower spatial specificity inherent in the volumetric measurements, which necessarily depend on the dimensions of a voxel as the unit of measurement. In the cortical thickness approach, measurements are iteratively made perpendicular to the cortical surface across its complex topography. Thus the average thickness in any given region is not dependent on a preset unit of measurement, but takes advantage of the greater precision of direct linear measurements.

The cortical thickness values in this study were similar to those obtained by other studies using the same methodology (Han et al., 2006; Kuperberg et al., 2003; Sailer et al., 2003). On average, the values from our healthy controls were higher compared to those of the unaffected hemisphere in patients (2.4 mm *vs* 2.1 mm in M1 and 1.9 mm *vs* 1.8 mm in V1) in agreement with a previous study that investigated the effect of aging on cortical thickness (Salat et al., 2004). It is important to point out that despite an indication of age-related thinning of the motor cortex, our study was based on within-subject hemispheral comparisons (paired *t*-test) and was not designed to investigate the relationship between aging and cortical thickness; age would not be expected to affect the brain asymmetrically. Our healthy younger participants confirmed a lack of an effect of handedness in the results obtained from the patient data.

5. Conclusion

Our study is the first to demonstrate hemispheral asymmetry in cortical thickness, controlled both by a within-patient comparison across different arterial territories, and by an independent set of healthy subjects. The cortical thinning in the brain region supplied by the carotid artery in the absence of frank stroke suggests a focal impact of regional cerebral hypoperfusion that warrants further investigation into the relationship of physiological and anatomical parameters in these regions. Our findings also provide validation of cortical thinning as a biomarker for vascular disease, a potentially useful clinical application.

References

Cheng, B., Schulz, R., Bönstrup, M., Hummel, F.C., Sedlacik, J., Fiehler, J., Gerloff, C., Thomalla, G., 2015. Structural plasticity of remote cortical brain regions is determined by connectivity to the primary lesion in subcortical stroke. J. Cereb. Blood Flow Metab.

Dale, A.M., Sereno, M.I., 1993. Improved localizadon of cortical activity by combining EEG and MEG with MRI cortical surface reconstruction: a linear approach. J. Cogn. Neurosci. 5, 162–176.

Dale, A.M., Fischl, B., Sereno, M.I., 1999. Cortical surface-based analysis: I. Segmentation and surface reconstruction. NeuroImage 9, 179–194.

Das, S.R., Avants, B.B., Pluta, J., Wang, H., Suh, J.W., Weiner, M.W., Mueller, S.G., Yushkevich, P.A., 2012. Measuring longitudinal change in the hippocampal formation from in vivo high-resolution T2-weighted MRI. NeuroImage 60, 1266–1279.

Desikan, R.S., Ségonne, F., Fischl, B., Quinn, B.T., Dickerson, B.C., Blacker, D., Buckner, R.L., Dale, A.M., Maguire, R.P., Hyman, B.T., 2006. An automated labeling system for subdividing the human cerebral cortex on MRI scans into gyral based regions of interest. NeuroImage 31, 968–980.

Duering, M., Righart, R., Wollenweber, F.A., Zietemann, V., Gesierich, B., Dichgans, M., 2015. Acute infarcts cause focal thinning in remote cortex via degeneration of connecting fiber tracts. Neurology 84, 1685–1692.

Fischl, B., Dale, A.M., 2000. Measuring the thickness of the human cerebral cortex from magnetic resonance images. Proc. Natl. Acad. Sci. 97, 11050–11055.

Fischl, B., Sereno, M.I., Dale, A.M., 1999. Cortical surface-based analysis: II: inflation, flattening, and a surface-based coordinate system. NeuroImage 9, 195–207.

Fischl, B., Liu, A., Dale, A.M., 2001. Automated manifold surgery: constructing geometrically accurate and topologically correct models of the human cerebral cortex. IEEE Trans. Med. Imaging 20, 70–80.

Fischl, B., Salat, D.H., Busa, E., Albert, M., Dieterich, M., Haselgrove, C., Van Der Kouwe, A., Killiany, R., Kennedy, D., Klaveness, S., 2002. Whole brain segmentation: automated labeling of neuroanatomical structures in the human brain. Neuron 33, 341–355.

Fischl, B., van der Kouwe, A., Destrieux, C., Halgren, E., Ségonne, F., Salat, D.H., Busa, E., Seidman, L.J., Goldstein, J., Kennedy, D., 2004. Automatically parcellating the human cerebral cortex. Cereb. Cortex 14, 11–22.

Fotiadis, P., van Rooden, S., van der Grond, J., Schultz, A., Martinez-Ramirez, S., Auriel, E., Reijmer, Y., van Opstal, A.M., Ayres, A., Schwab, K.M., 2016. Cortical atrophy in patients with cerebral amyloid angiopathy: a case-control study. Lancet Neurol. 15, 811–819.

Geisseler, O., Pflugshaupt, T., Bezzola, L., Reuter, K., Weller, D., Schuknecht, B., Brugger, P., Linnebank, M., 2016. Cortical thinning in the anterior cingulate cortex predicts multiple sclerosis patients' fluency performance in a lateralised manner. NeuroImage Clin. 10, 89–95.

Han, X., Jovicich, J., Salat, D., van der Kouwe, A., Quinn, B., Czanner, S., Busa, E., Pacheco, J., Albert, M., Killiany, R., 2006. Reliability of MRI-derived measurements of human cerebral cortical thickness: the effects of field strength, scanner upgrade and manufacturer. NeuroImage 32, 180–194.

Harrison, T.M., Mahmood, Z., Lau, E.P., Karacozoff, A.M., Burggren, A.C., Small, G.W., Bookheimer, S.Y., 2016. An Alzheimer's disease genetic risk score predicts longitudinal thinning of hippocampal complex subregions in healthy older adults. Eneuro 3 (ENEURO. 0098-0016.2016).

Hwang, J., Kim, C.M., Jeon, S., Lee, J.M., Hong, Y.J., Roh, J.H., Lee, J.-H., Koh, J.-Y., Na, D.L., Initiative, A.s.D.N., 2016. Prediction of Alzheimer's disease pathophysiology based on cortical thickness patterns. Alzheimers Dement: Diagnosis, Assessment & Disease Monitoring 2, 58–67.

Jehna, M., Pirpamer, L., Khalil, M., Fuchs, S., Ropele, S., Langkammer, C., Pichler, A., Stulnig, F., Deutschmann, H., Fazekas, F., 2015. Periventricular lesions correlate with cortical thinning in multiple sclerosis. Ann. Neurol. 78, 530–539.

Kuperberg, G.R., Broome, M.R., McGuire, P.K., David, A.S., Eddy, M., Ozawa, F., Goff, D., West, W.C., Williams, S.C., van der Kouwe, A.J., 2003. Regionally localized thinning of the cerebral cortex in schizophrenia. Arch. Gen. Psychiatry 60, 878–888.

Reuter, M., Schmansky, N.J., Rosas, H.D., Fischl, B., 2012. Within-subject template estimation for unbiased longitudinal image analysis. NeuroImage 61, 1402–1418.

Rosas, H.D., Liu, A.K., Hersch, S., Glessner, M., Ferrante, R.J., Salat, D.H., van der Kouwe, A., Jenkins, B.G., Dale, A.M., Fischl, B., 2002. Regional and progressive thinning of the cortical ribbon in Huntington's disease. Neurology 58, 695–701.

Rosas, H., Liu, A., Hersch, S., Glessner, M., Ferrante, R., Salat, D., van Der Kouwe, A., Jenkins, B., Dale, A., Sailer, M., Fischl, B., Salat, D., Tempelmann, C., Schönfeld, M.A., Busa, E., Bodammer, N., Heinze, H.J., Dale, A., 2003. Focal thinning of the cerebral cortex in multiple sclerosis. Brain 126, 1734–1744.

Sailer, M., Fischl, B., Salat, D., Tempelmann, C., SchoÈnfeld, M.A., Busa, E., Bodammer, N., Heinze, H.J., Dale, A., 2003. Focal thinning of the cerebral cortex in multiple sclerosis. Brain 126, 1734–1744.

Salat, D.H., Buckner, R.L., Snyder, A.Z., Greve, D.N., Desikan, R.S., Busa, E., Morris, J.C., Dale, A.M., Fischl, B., 2004. Thinning of the cerebral cortex in aging. Cereb. Cortex 14, 721–730.

Ségonne, F., Dale, A., Busa, E., Glessner, M., Salat, D., Hahn, H., Fischl, B., 2004. A hybrid approach to the skull stripping problem in MRI. NeuroImage 22, 1060–1075.

Ségonne, F., Pacheco, J., Fischl, B., 2007. Geometrically accurate topology-correction of cortical surfaces using nonseparating loops. IEEE Trans. Med. Imaging 26, 518–529.

Shaw, M.E., Abhayaratna, W.P., Sachdev, P.S., Anstey, K.J., Cherbuin, N., 2016. Cortical thinning at midlife: the PATH through life study. Brain Topogr. 1–10.

Sled, J.G., Zijdenbos, A.P., Evans, A.C., 1998. A nonparametric method for automatic correction of intensity nonuniformity in MRI data. IEEE Trans. Med. Imaging 17, 87–97.